

1 **Production of more sustainable emulsions formulated with eco-friendly materials**

2 Mario Fresneda^a, Luis A. Trujillo-Cayado^a, M Carmen García^a, Maria-Carmen Alfaro-
3 Rodriguez^{a*} and José Muñoz^a.

4 ^aDepartamento de Ingeniería Química, Facultad de Química, Universidad de Sevilla, C/
5 P. García González, 1, E41012, Sevilla, Spain.

6 * Corresponding author: Maria-Carmen Alfaro-Rodriguez; Tel.: +34 954 557180; fax:
7 +34 954 556447; *E-mail address*: alfar@us.es

8

9 **Abstract**

10 Sustainable development involves the search for new products with a low environmental
11 impact. Hence, the aim of this work is to obtain stable and concentrated aqueous
12 emulsions containing bitter fennel oil and a biomass-derived emulsifier by studying
13 different processing variables and techniques. Firstly, the effects of the application of a
14 premix step previous to homogenization and of the geometry of the high-energy rotor-
15 stator device used (Silverson L5M or Ultraturrax T50) on the droplet size distribution
16 (DSD) and physical stability (PS) of emulsions were investigated. The use of a premix
17 worsens both the physical stability and the average droplet diameters of the emulsions,
18 the most stable emulsion being that obtained with the Silverson L5M alone. Secondly,
19 the stability of this emulsion was improved. To achieve this goal, this coarse emulsion
20 was microfluidized at different pressures (from 5000 to 25000 psi), reaching submicron
21 sizes and monomodal distributions, except for that subjected to 25000 psi which resulted
22 in clear overprocessing. Creaming and oiling off were the main destabilization processes.
23 The emulsion exhibiting the lowest droplet sizes and the best physical stability was
24 prepared at 20000 psi. This work contributes to the development of sustainable
25 agrochemical prototypes.

26

27 **Keywords:** Bitter fennel oil, Wheat derived surfactant, Emulsion, Premix in primary
28 homogenization, Microfluidizer, Physical stability.

29 **Introduction**

30 In order to reduce both human health and environmental risks, scientists have a great
31 effort to work out future strategies with respect to green chemistry (Durand et al., 2016).

32 One of them is the incorporation of eco-friendly materials in the design of new products.

33 For this reason, sustainability has become an important requirement for solvents, leading
34 to the need to develop new green solvents. The non-polar characteristic of some of these

35 organic solvents means that they cannot be dispersed directly in another aqueous phase
36 (Israelachvili, 2011). Hydrophobic compounds could be incorporated as functional or

37 active ingredients in a wide variety of colloidal systems with application in sectors such
38 as food or agrochemicals. An important application of this type of system in the field of

39 agrochemicals is the use of emulsions of essential oils, which can be used as a matrix for
40 pesticides, where the essential oil functions as a solvent friendly to the environment. In

41 previous works, emulsions containing essential oils such as alpha-pinene (García et al.,
42 2014; García et al., 2015), limonene (Trujillo-Cayado et al., 2016) or thyme essential oil

43 (Martin et al., 2018) were studied for this purpose.

44 Another important issue is that the fact of considering the use of the biodegradable raw
45 materials leads to obtaining both a final product with little impact on the environment and

46 waste which is less harmful to it (Bom et al., 2019). As indicated Saéz-Martinez et al
47 (2016) the future must be made up of green, sustainable and recyclable chemicals. In the

48 present work, in order to achieve this purpose, emulsions containing bitter fennel essential
49 oil as an ecological solvent were produced. The bitter fennel plant is a common perennial

50 hemicryptophyte from the Mediterranean basin whose main components are estragole

51 and trans-anethole in addition to the cyclic monoterpenes of fenchone and limonene
52 (Gross et al, 2002).

53 Frequently, essential oils have been utilized as natural preservatives and as fragrances in
54 cosmetic products, but as a result of their antimicrobial and antioxidant properties, new
55 applications are emerging for them in sectors such as food or agriculture (Rodríguez-Rojo
56 et al., 2012). Their hydrophobicity, as mentioned above, makes many of their applications
57 difficult, although it is their volatility that supposes a greater barrier (Llinares et al., 2018).
58 One way to reduce this problem is the formulation of stable emulsions that reduce
59 evaporation (Rodríguez-Rojo et al., 2012). Oil-in-water emulsions are one of the main
60 components of many commercial products. Currently, this type of emulsion can be found
61 in foods, vitamin supplements, drugs, cosmetics, personal care items and agrochemicals.
62 However, emulsions are, from a thermodynamic point of view, extremely unstable and
63 the two phases that compose them tend to separate (Borwankar et al., 1992). For this
64 reason, other components such as surfactants, proteins or thickeners are commonly used
65 to improve emulsion stability, with the use of the surfactant playing an important role in
66 this. The surfactant molecules tend to position themselves at the interface produced
67 between the dispersed oil droplets and the aqueous continuous phase (Dickinson et al.,
68 1989). Thus, several processes involved in emulsion destabilization are controlled by the
69 presence of the surfactant, which influences electrostatic and steric repulsion and
70 consequently, the emulsion stability (McClements, 2007). For this purpose, Applyclean
71 6548 has been employed as emulsifier. It is a non-ionic surfactant derived from wheat
72 which belongs to the family of alkyl poly pentosides (APP). This surfactant has all the
73 necessary characteristics to be considered as an ecological surfactant, since it derives from
74 a renewable source and its production is carried out by means of a process that respects
75 the environment (Trujillo-Cayado et al., 2018). In fact, this surfactant, developed by the

76 French company Wheatoleo, has ECOCERT certification. Its main characteristics include
77 its low toxicity, its rapid biodegradation and its HLB, which is between 9.0 and 9.5. In
78 addition, it should be noted that the use of this surfactant, which is obtained from wheat
79 straw, avoids the waste accumulation in the environment and converts these wastes into
80 added-value materials. Furthermore, as Lin et al (2013) point out, its raw material does
81 not compete with food production.

82 Another point to take into account to increase of these emulsions sustainability is the use
83 of the most friendly production strategy. This is to say to perform a cleaner production in
84 which the environmental contamination is reduced as Krolczyk et al. purposed in a
85 previous work (Krolczyk et al., 2017). Recent works have carried out this aim centering
86 their studies in ecological procedures (Mia, et al., 2018). It should be noted that today it
87 is so important to provide solutions for environmental degradation that there are
88 numerous studies that are being developed related to sustainable production. Among the
89 most recent ones, the one carried out by Correa et al. (2019) for the biofuel production,
90 the study of Nidheesh and Kumar (2019) for the cement and steel production or that of
91 Mark et al. (2019) for the production of phenolic compounds. In this way, Bom et al.,
92 (2019) in their review about sustainability in the cosmetic industry considered several
93 processing variables such as the use of the same equipment in process in which several
94 steps are involved, the production energy optimization, the reduction of the washing
95 water, etc. The same points can be used in other industries. In addition, it is worth making
96 an effort to find out the devices which produce less impact on the environment. As
97 Krolczyk et al (2019), reported, this fact can be the opener for a cleaner and friendly
98 production. For this purpose, the main objective of this work is to evaluate different
99 processing conditions to produce an environmentally friendly emulsion from a mixture
100 whose main components are bitter fennel essential oil and water, in order to select the
101 most sustainable processing protocol that provides greater emulsion stability. Firstly, the
102 influence of a premix stage in the processing of oil-of-fennel-in-water emulsions was
103 studied. For this, four experiments were carried out. On the one hand, two systems were
104 subjected to a premixing process with a low-energy rotor-stator equipment prior to the
105 emulsification with high-energy rotor-stator devices (two different geometries) and on
106 the other hand, two systems in which the emulsification was carried out directly, without

107 any type of premix. The importance of this stage of the study lies in determining the
108 number of steps of the most sustainable processing. Subsequently, the stability of the
109 emulsions obtained as a function of aging time was studied by means of laser diffraction
110 and multiple light scattering techniques. The most stable emulsion produced during this
111 stage was then improved with the microfluidization equipment (Microfluidizer M-110P).
112 The influence of pressure on its properties was analyzed. In this way, the optimal
113 processing conditions were established for the emulsification of a mixture whose main
114 elements are bitter fennel essential oil, wheat biomass-derived surfactant and water which
115 could be used as a prototype for sustainable agrochemicals. An analysis of both
116 processing variables led to the optimization of the processing protocol in order to achieve
117 the most respectful with the environment.

118 **Materials and methods**

119 *Materials*

120 Bitter fennel essential oil (density: 0.897 Kg/m³) kindly supplied by Destilaciones Bordas
121 Chinchurreta S.A was used as dispersed phase. Applyclean 6548 (D-xylofuranose,
122 oligomeric tetradecyl and octodecyl glycoside, C14, C18 alcohol) (Martín et al., 2018),
123 produced by Wheatoleo, was utilized as emulsifier. In order to preserve the emulsions,
124 sodium azide (Panreac) was included. Milli- Q water was used to complete the
125 formulation.

126 Studied emulsions contained 40 wt% oil phase, 4 wt% surfactant, 0.1 wt% sodium azide
127 and Milli- Q water as continuous phase.

128 *Preparation of emulsions*

129 The continuous phase was prepared by mixing the necessary amount of sodium azide in
130 Milli-Q water at room temperature by means of a magnetic stirring plate (SM 162, Stuart,
131 Scientific Laboratory Supplies). Subsequently, the dispersed phase was obtained by

132 dissolving the appropriate quantity of Applyclean 6548 in bitter fennel essential oil at
133 70°C for 15 minutes. For this purpose, a Phoenix (Thermo-Scientific) bath was employed.

134 Once both dispersed and continuous phases were prepared, four different emulsions were
135 obtained using the following protocols:

136 1. IKA-UT50 emulsion. These emulsions were produced by adding the dispersed
137 phase to the continuous phase at 400 rpm for one minute using an IKA-VISC MR-
138 D1 low-energy rotor-stator homogenizer (IKA Labortechnik, Germany) and then
139 continuing for one additional minute at the same rate. This emulsion was
140 immediately homogenized with a high speed rotor-stator homogenizer
141 (Ultraturrax T50) at 2000 rpm for one minute and then 30 s at 6000 rpm.

142 2. IKA-SL5M emulsion. The process used in this case was similar to that of the
143 previous emulsion. In this protocol, a Silverson L5M rotor-stator homogenizer
144 was utilized instead of the Ultraturrax T50.

145 3. UT50 emulsion. The dispersed phase was added to the aqueous phase for 1 minute
146 at 2000rpm by means of the Ultraturrax T50 homogenizer. Lastly, 6000 rpm for
147 30 s was applied as a final homogenization.

148 4. SL5M emulsion. The processing protocol was similar to the UT50 emulsion, but
149 the equipment used was Silverson L5M.

150 In a further stage, the most stable emulsion produced during the first stage was submitted
151 to a second homogenization process by means of Microfluidizer M-110P (Microfluidics,
152 EEUU). In this equipment, batches of 200 g were processed at different pressures (5000
153 psi, 10000 psi, 15000 psi, 20000 psi and 25000 psi).

154 At least two samples were prepared with every protocol.

155 *Emulsion characterization*

156 *Laser diffraction*

157 This technique was employed to determine the droplet size distribution. For this purpose,
158 a Mastersizer 2000 (Malvern, Uk) was used. Milli-Q water was utilized as the dispersant
159 medium. The refraction index was 1.54 for the oil dispersed phase and the refraction and
160 adsorption indexes for the aqueous medium were 0.5 and 1.33, respectively.

161 In order to analyse the influence of the processing protocols on the mean droplet
162 diameters, Sauter diameter ($D[3,2]$) and volume mean diameter ($D[4,3]$) have been
163 employed. These parameters are defined as following:

164
$$D[3,2] = \frac{\sum_{i=1}^N n_i d_i^3}{\sum_{i=1}^N n_i d_i^2}$$

165
$$D[4,3] = \frac{\sum_{i=1}^N n_i d_i^4}{\sum_{i=1}^N n_i d_i^3}$$

166 where N is the total number of droplets, d_i is the droplet diameter and n_i is the number of
167 droplets having a diameter d_i .

168 To find out the distribution width of droplet sizes distribution, the “span” was used, which
169 was determined as follows:

170
$$Span = (D[v,0.9] - D[v,0.1]) / D[v,0.5]$$

171 where $D[v, 0.9]$ and $D[v, 0.1]$ stand for the 90th and 10th percentiles and $D[v, 0.5]$ for the
172 median.

173 In order to study the emulsion stability, these measurements were performed at 1 day, 5
174 days and 14 days of aging time.

175 At least two replicates of each test were performed at room temperature.

176 *Multiple light scattering*

177 Turbiscan Lab (Formulation, France) was used to evaluate the physical stability of the
178 emulsions obtained. Tests were carried out at room temperature. Turbiscan determines
179 backscattering and transmission as a function of the length of the cell containing the
180 sample, but in this work only backscattering is presented as a consequence of the fact that
181 the transmission values recorded were null.

182 **Results and discussion**

183 *Influence of the premix and the high-energy rotor-stator device used on the*
184 *microstructure and physical stability of emulsions*

185 Figure 1 shows the influence of the processing protocols on the droplet size distribution
186 of the emulsions containing bitter fennel essential oil as dispersed phase after 24 hours of
187 aging. Monomodal distributions with a peak at around 2.5 μm , were exhibited for all the
188 emulsions produced. As can be observed, emulsions obtained with a previous
189 homogenization step presented a droplet size distribution centred on higher droplet sizes.
190 This could be a result of a re-coalescence mechanism related to an excess of applied
191 energy which could have provoked the breaking of several droplets. This fact led to the
192 displacement of the curve towards higher diameters and, therefore, to emulsions with
193 larger droplets sizes (Jafari et al., 2008; García et al. 2016). In addition, the emulsions
194 obtained with the Silverson L5M equipment showed droplet size distributions displaced
195 towards smaller diameters than those prepared by means of Ultraturrax T50. This result
196 had already been observed in a previous work (Trujillo-Cayado et al., 2018). Although,
197 under the same operation conditions, the Ultraturrax T50 device applies higher energy
198 than Silverson L5M, the latter is more effective, probably due to the geometry of the rotor
199 used. This finding was supported by the mean diameter values and the standard deviations
200 exhibited in Table 1. Therefore, the best results were presented by emulsions obtained

201 only using Silverson 5M. From a sustainable production point of view this result is very
202 important since involves an energy reduction and higher production efficiency (Alayón
203 et al., 2017)

204 By way of example, Figure 2 illustrates the evolution of droplet size distribution with
205 aging time for the emulsion developed by IKA-SL5M processing. As can be observed,
206 there was no significant changes in the mean droplet sizes and, therefore, there was no
207 destabilization by coalescence or Ostwald ripening during the evaluation time. The same
208 result was obtained for the other emulsions investigated. This fact revealed that
209 Appyclean 6548 perfectly fulfills its role as an emulsifier since not only made it possible
210 to obtain concentrated emulsions, but that it was also able to satisfactorily cover the
211 oil/water interface protecting it against the rupture.

212 The emulsion stability was assessed by multiple light scattering monitoring for at least 27
213 days. All emulsions showed similar results with a decrease in the backscattering with the
214 aging time at the bottom and at the top of the vessel containing the sample, which is
215 coherent with the existence of a destabilization mechanism by creaming and oiling off,
216 respectively (McClements, 2015). There was no change in the backscattering in the
217 middle of the measuring cell which demonstrated droplets sizes remained invariable
218 (Mengual et al., 1999). This result is in agreement with that obtained from the laser
219 diffraction technique. In Figure 3, the backscattering evolution over the whole of the
220 container height as a function of the aging time is shown for one selected emulsion, IKA-
221 SL5M. Additionally, in order to compare the different emulsions studied and better
222 visualize the changes produced, in Figure 4 the backscattering in reference mode (Δ BS)
223 of these emulsions at 27 days of aging time as function of the measuring cell length is
224 shown. This figure supports the analysis above, namely all emulsions suffered similar
225 effects, a marked decrease in the Δ BS at the bottom as a consequence of a creaming

226 process and a slight decrease in ΔBS at the top due to an oiling off destabilization
227 phenomenon. This last phenomenon appears by coalescence of droplets of cream phase
228 (Mengual et al., 1999) which provokes the occurrence of this oil layer at the top of the
229 vessel.

230 The destabilization kinetic of the creaming process, the creaming index (IC)
231 (McClements, 2007), as a function of the aging time has been calculated by the following
232 equation (1):

$$233 \quad CI(\%) = \frac{H_S}{H_E} \cdot 100 \quad (1)$$

234 where CI is the creaming index, H_S is the creaming layer length and H_E is the sample
235 length. CI as a function of the aging time is plotted in Figure 5. The creaming rate, ω , has
236 been determined from this figure by means of equation 2 (Trujillo-Cayado et al., 2017):

$$237 \quad \omega = \frac{d(CI)}{dt} \cdot \frac{H_E}{100} \quad (2)$$

238 As can be observed in Figure 5, SL5M emulsion presented a lower slope and, as a
239 consequence, a lower creaming rate $\omega = 0.182$ %/day. This value contrasts, for example,
240 with that obtained for IKA-SL5M and UT50 emulsions which showed a creaming rate of
241 0.218 and 0.698 %/day, respectively, being this last obtained from the linear part of the
242 curve, that is to say, during the first 200 hours of study. This fact reveals SL5M emulsion
243 showed the lowest destabilization due to creaming. It must be taken into account that the
244 destabilization by creaming is strongly affected by the medium viscosity and the size and
245 polydispersity of the droplets. In these emulsions, large sizes and span values are reached,
246 as is supported in Table 1.

247 To quantify all the possible destabilization processes that occur in the emulsions
248 simultaneously, a parameter called "Turbiscan Stability Index" (TSI) obtained from
249 equation (3) has been used (Xu et al., 2016):

$$250 \quad TSI = \sum_i \frac{\sum_h |scan_i(h) - scan_{i-1}(h)|}{H} \quad (3)$$

251 Where $scan_i(h)$ is the average backscattering for each time (i) of measurement, $scan_{i-1}(h)$
252 is the average backscattering for the (i-1) time of measurement and H is the number of
253 scans carried out on the sample. As can be deduced from this equation, a higher value of
254 TSI means a lower stability.

255 The TSI values as a function of the aging time have been plotted in Figure 6. The lowest
256 value of this parameter at 27 days is exhibited by the SL5M emulsion, this being,
257 therefore, the most stable emulsion.

258 As a consequence of the results obtained in this section, the emulsion obtained using only
259 the Silverson L5M device will be used as the primary emulsion, namely as the starting
260 point, for the next study.

261 From the environmental point of view, interesting finding can be noted. On the one hand,
262 the elimination of the premix stage leads to a substantial saving in energy consumption.
263 And the other hand, this fact provokes an important reduction in washing water.

264 *Influence of the pressure on the microstructure and physical stability of microfluidized* 265 *emulsions*

266 In this part of the work, the most stable emulsion obtained previously, SL5M, was used
267 as the primary emulsion to feed a M110P Microfluidizer homogenizer and was submitted
268 to different pressures. The pressures applied ranged from 5000 to 25000 psi.

269 Laser diffraction results were obtained 24 hours after their production and are shown in
270 Figure 7. As can be observed in Figure 7 and Table 2, the droplet sizes of microfluidized

271 emulsions were much smaller than those processed only with a rotor-stator system, with
272 or without premix.

273 The small sizes zone of droplet size distribution tends to move towards smaller diameters
274 and, therefore, to decreased mean Sauter diameters as the applied pressure increases in
275 the range of 5000-20000 psi. The emulsion prepared at 25000 psi had higher $D_{3,2}$ values
276 than for the emulsion processed at 20000 psi. In addition, from 15000 psi the distributions
277 become bimodal, being monomodal only in the range 5000-10000 psi. Furthermore, the
278 high sizes zone of DSD shifts to higher values. As result of these facts, the mean volume
279 diameter and span significantly increase at the highest pressures. This could be due to the
280 fact that, from these pressures, although drops of smaller diameters are formed, an over-
281 processing is produced in other droplets which causes recoalescence and, as a
282 consequence, the formation of a distribution tending to larger sizes (García et al., 2016;
283 Trujillo-Cayado et al., 2018).

284 Figure 8 shows, by way of example, the droplet size distribution as a function of the aging
285 time for the emulsion obtained at 20000 psi. As can be observed, there was a slight
286 displacement of the distribution toward higher droplets sizes. However, these differences
287 were not significant, as can be deduced from the comparison of Sauter diameters and their
288 standard deviation at 1 day and 14 days which were $D_{3,2} = 0.52 \pm 0.02 \mu\text{m}$ and $D_{3,2} = 0.54$
289 $\pm 0.02 \mu\text{m}$, respectively. Additionally, Figure 9, where the physical stability is analyzed
290 by multiple light scattering, exhibits only a slight variation in ΔBS in the middle of the
291 vessel at 55 days, which again indicates that this slight coalescence or Ostwald ripening
292 process was not important. Therefore, Figure 9 also demonstrates that there was no
293 change in the droplet size. This statement can be extrapolated to all microfluidized
294 emulsions. In contrast, the emulsions submitted to pressure exhibited destabilization by

295 creaming and oiling off similarly to the primary emulsion, despite having much smaller
296 mean droplet sizes. In any case, the peak (decrease of ΔBS at the bottom) is of lower
297 width for emulsions submitted to microfluidization. The higher study time for the latter
298 emulsions (55 days against 27 days) should be noted. Regarding these emulsions, the one
299 with the least destabilization by creaming (least intensity and width in the
300 abovementioned peak) corresponds to the emulsion prepared at 20000 psi, which is the
301 one with the lowest average Sauter diameter.

302 Figure 10 shows the creaming index versus aging time for every microfluidized emulsion.
303 As can be observed, after a delay period, a linear dependence of the creaming index with
304 time occurred. From the slope of this region, it is possible to obtain the creaming rate (ω)
305 and, therefore, the gravitational separation resistance. Table 3 exhibits the creaming rate
306 (ω) and the time of creaming onset ($t_{0,c}$). As can be observed in this table, the emulsions
307 obtained at 15000 psi and 20000 psi exhibited the lower creaming rate, and therefore were
308 the more stable emulsions against creaming, although among them, the most stable
309 emulsion is the one processed at 20000 psi due to the fact that the creaming destabilization
310 starts later. This result is in agreement to results obtained by laser diffraction. The more
311 stable emulsions in relation to the creaming effect were those with smaller drop sizes
312 (15000 and 20000 psi) (McClements, 2015). It should be noted that in all cases, the values
313 of ω were much lower than the values obtained for the primary emulsion, the emulsion
314 that did not have a stage of secondary homogenization at high pressure (SL5M).

315 In Figure 11 the TSI values are plotted against the aging time for the microfluidized
316 emulsions. It is again shown that the most stable emulsion is that prepared at 20000 psi.
317 This emulsion exhibited not only the lowest level of creaming but also the lowest level of
318 oiling off, as illustrated in Figure 9. As can be previously observed, the emulsions

319 obtained at 25000 psi exhibited a faster destabilization by creaming process than those of
320 15000 psi and 20000 psi as a consequence of its higher droplet size. This fact was
321 consistent with the results presented in Figure 11. It is noteworthy again that the values
322 of TSI, in all cases, were much lower than those shown by the emulsions from the first
323 part of the study, even taking into account that in these emulsions the aging time was
324 much longer.

325

326 **Conclusions**

327 Concentrated O/W emulsions containing 40 wt% bitter fennel oil and a bio-derived
328 surfactant (Appyclean 6548, 4 wt %) were obtained. From an environmental point of
329 view, these emulsions exhibit several advantages: a) they are aqueous based formulations
330 which facilitates its application b) they are concentrated which provides savings in the
331 transportation c) they are formulated with friendly raw materials which causes that the
332 resulting wastes are less harmful. All these facts contribute to reduce the impact on the
333 environment. Along with the formulation, other point must be taken into account which
334 is the production procedure. Firstly, the influence of the incorporation of a premix stage
335 prior to homogenization on the droplet size distribution and physical stability of the
336 emulsions was investigated. The results obtained showed that the use of a premix worsens
337 the physical stability of the emulsions and increases the average droplet diameters as a
338 consequence of re-coalescence due to excessive mechanical energy and to the entry of pre-
339 existing droplets into the rotor-stator system. This finding contributes to an important
340 saving in the energy consumption and the washing water and, therefore, a more
341 sustainable production. The best results were obtained for the emulsion prepared only
342 with Silverson L5M which, at the same speed, consumes less energy leading to a more

343 efficient energy process. All the emulsions developed in the first part of the investigation
344 had mean droplet sizes greater than one micron, as well as destabilization by creaming
345 and oiling off. The creaming rate and the physical stability of the emulsions are directly
346 related to the droplet sizes. For this reason, the most stable emulsion and the one that
347 presented the least destabilization by creaming was that which had the lowest average
348 diameters that obtained only by means of Silverson L5M, without premix. Subsequently,
349 the influence of homogenization pressure (between 5000 and 25000 psi) on the Silverson
350 L5M emulsion was studied in a high energy microfluidization system, Microfluidizer
351 M110P. These emulsions had submicron droplet sizes, much lower than any of those
352 obtained in the first part and, as a result of this, better physical stability. The mean
353 diameters and the turbiscan stability index decreased as the pressure increased in the range
354 of 5000-20000 psi. The emulsion processed at 25000 psi showed larger diameters and, as
355 a consequence, worse physical stability, probably due to a recoalescence process induced
356 by an excess of energy. Thus, the emulsion that had smaller droplet sizes, as well as
357 greater physical stability, was that prepared at 20000 psi.

358 As above mentioned, this work contributes to the development of stable agrochemical
359 prototypes which are sustainable. These emulsions are sustainable not only by their
360 formulation, based on essential oil and wheat waste surfactant but also by their processing
361 protocol which could be conducive to a reduction of the impact on the environment.

362 **Acknowledgements**

363 The financial support received (Project CTQ2015-70700-P) from the Spanish Ministerio
364 de Economía y Competitividad and from the European Commission (FEDER
365 Programme) is kindly acknowledged.

366

367 **Conflicts of Interest:** The authors declare no conflict of interest.

369 **Literature cited**

370 Alayón, C., Säfsten, K., Johansson, G. Conceptual sustainable production principles in
371 practice: Do they reflect what companies do? *Journal of Cleaner Production* 141 (2017)
372 693-701. <https://doi.org/10.1016/j.jclepro.2016.09.079>.

373

374 Borwankar, R.P., Lobo, L. A., Wasan, D. T. Emulsion stability-kinetics of flocculation
375 and coalescence, *J. Colloid Interface Sci.* 69 (1992) 135-146.
376 [https://doi.org/10.1016/0166-6622\(92\)80224-P](https://doi.org/10.1016/0166-6622(92)80224-P).

377

378 Correa, D. F., Beyer, H. L., Fargione, J. E., Hill, J. D., Possingham, H. P., Thomas-Hall,
379 S. R., & Schenk, P. M. Towards the implementation of sustainable biofuel production
380 systems. *Renewable and Sustainable Energy Reviews* 107 (2019) 250-263.
381 <https://doi.org/10.1016/j.rser.2019.03.005>.

382

383 Dickinson, E., Woskett, C.C, in: R.D. Bee, P. Richmond, Mingins, J. (Eds), *Food*
384 *Colloids*, Royal Society of Chemistry, London, 1989.

385 Durand, E., Lecomte, J., & Villeneuve, P. From green chemistry to nature: The versatile
386 role of low transition temperature mixtures. *Biochimie*, 120 (2016) 119–123. Doi:
387 <https://doi.org/10.1016/j.biochi.2015.09.019>

388 García, M.C., Alfaro, M.C., Calero, N., Muñoz, J. Influence of polysaccharides on the
389 rheology and stabilization of α -pinene emulsions. *Carbohydr. Polym.* 105 (2014) 177–
390 183. <http://dx.doi.org/10.1016/j.carbpol.2014.01.055>.

391

392

393 García, M.C., Alfaro, M.C., Muñoz, J. Influence of the ratio of amphiphilic copolymers
394 used as emulsifiers on the microstructure, physical stability and rheology of α -
395 pinene emulsions stabilized with gellan gum. *Colloids and Surfaces B: Biointerfaces*
396 135 (2015) 465–471. <http://dx.doi.org/10.1016/j.colsurfb.2015.07.060>.

397

398 García, M.C., Muñoz, J., Alfaro, M.C., Franco, J.M. Influence of Processing on the
399 Physical Stability of Multiple Emulsions Containing a Green Solvent *Chem. Eng.*
400 *Technol.* 39 (2016) 6, 1137–1143. <http://dx.doi.org/10.1002/ceat.201500283>.

401

402

403 Gross, M., Friedman, J., Dudai, N., Larkov, O., Cohen, Y., Bar, E., Lewinsohn, E.
404 Biosynthesis of estragole and t-anethole in bitter fennel (*Foeniculum vulgare* Mill. var.
405 *vulgare*) chemotypes. Changes in SAM: phenylpropene O-methyltransferase activities

406 during development. *Plant Science*, 163 (2002), 1047–1053.
407 [https://doi.org/10.1016/S0168-9452\(02\)00279-0](https://doi.org/10.1016/S0168-9452(02)00279-0).

408

409 Israelachvili, J. *Intermolecular and Surface Forces*. [https://doi.org/10.1016/C2009-0-](https://doi.org/10.1016/C2009-0-21560-1)
410 [21560-1](https://doi.org/10.1016/C2009-0-21560-1), Academic Press, 2011.

411 Jafari, S. M., Assadpoor, E., He, Y., & Bhandari, B. Re-coalescence of emulsion droplets
412 during high-energy emulsification. *Food Hydrocolloids*, 22 (2008) 1191–1202.
413 <https://doi.org/10.1016/J.FOODHYD.2007.09.006>.

414

415 Krolczyk, G. M., Maruda, W., Krolczyk, J.B., Wojciechowski, S., Mia, M., Nieslony,
416 P., Budzik, G. Ecological trends in machining as a key factor in sustainable production
417 – A review. *Journal of Cleaner Production*, 218 (2019), 601-615.
418 <https://doi.org/10.1016/j.jclepro.2019.02.017>

419 Krolczyk, G. M., Nieslony, P., Maruda, R. W., Wojciechowski, S. Dry cutting effect in
420 turning of a duplex stainless steel as a key factor in clean production. *Journal of Cleaner*
421 *Production*, 142 (2017) 3343-3354.

422 Llinares, R., Ramírez, P., Carmona, J., Carrillo, F., Muñoz, J. Formulation and
423 optimization of emulsions based on bitter fennel essential oil and EO/BO block
424 copolymer surfactant. *Colloids Surf., A*. 536 (2018), 142–147.
425 <https://doi.org/10.1016/j.colsurfa.2017.07.027>.

426 Lin, C.S.K., Pfaltzgraff, L.A., Herrero-Davila, L., Mubofu, E.B., Abderrahim, S., Clark,
427 J.H., Koutinas, A., Kopsahelis, N., Stamatelatos, K., Dickson, F., Thankappan, S.,
428 Mohamed, Z., Brocklesby, R., Luque, R. Food waste as a valuable resource for the
429 production of chemicals, materials and fuels. Current situation and global perspective.
430 *Energy Environ. Sci.* 6 (2013), 426-464

431

432 Mark, R., Lyu, X., Lee, J. J., Parra-Saldívar, R., & Chen, W. N. Sustainable production
433 of natural phenolics for functional food applications. *Journal of Functional Foods*
434 57(2019) 233-254. <https://doi.org/10.1016/j.jff.2019.04.008>

435

436 Martín, M.J., Trujillo, L.A., García, M.C., Alfaro, M.C., Muñoz, J. Effect of emulsifier
437 HLB and stabilizer addition on the physical stability of thyme essential oil emulsions. *J.*
438 *Dispersion Sci. Technol.* 39 (2018) 11, 1627-1634.
439 <https://doi.org/10.1080/01932691.2018.1459677>

440

441 McClements, D. J. (2015). *Food emulsions* (3rd Editio). Boca Ratón: CRC Press.
442 [http://www.cabdirect.org/abstracts/19910445562.html;jsessionid=F1B238C4FB6F0D64](http://www.cabdirect.org/abstracts/19910445562.html;jsessionid=F1B238C4FB6F0D642B12BC92C9788F1A?freeview=true)
443 [2B12BC92C9788F1A?freeview=true](http://www.cabdirect.org/abstracts/19910445562.html;jsessionid=F1B238C4FB6F0D642B12BC92C9788F1A?freeview=true).

- 444 McClements, D. J. Critical Review of Techniques and Methodologies for
445 Characterization of Emulsion Stability, *Crit. Rev. Food Sci. Nutr.*, 47 (2007) 611–649.
446 DOI: [10.1080/10408390701289292](https://doi.org/10.1080/10408390701289292).
- 447 Mengual, O., Meunier, G., Cayre, I., Puech, K., Snabre, P. Characterisation of instability
448 of concentrated dispersions by a new optical analyser: the TURBISCAN MA 1000.
449 *Colloids Surf., A*, 152 (1999) 111-123.
- 450 Mia, M., Gupta, M.K., Singh, G., Królczyk, G., Pimenov, D.Y. An approach to cleaner
451 production for machining hardened steel using different cooling-lubrication conditions.
452 *J. Clean. Prod.*, 187 (2018), 1069–1081. Doi:
453 <https://doi.org/10.1016/j.jclepro.2018.03.279>
- 454 Rodríguez-Rojo, S., Varona, S., Nuñez, M, Cocero, M.J. Characterization of Rosemary
455 essential oil for biodegradable emulsions. *Industrial Crops and Products* 37 (2012) 137-
456 140. <https://doi.org/10.1016/j.indcrop.2011.11.026>.
- 457 Sáez-Martínez F. J., Lefebvre, G., Hernández, J. J., & Clark, J. H. Z, Francisco J. Drivers
458 of sustainable cleaner production and sustainable energy options. *Journal of cleaner*
459 *production*, 138 (2016) 1-7.
- 460 Trujillo-Cayado, L. A., Alfaro, M. C., & Muñoz, J. (2018). Effects of ethoxylated fatty
461 acid alkanolamide concentration and processing on d-limonene emulsions. *Colloids and*
462 *Surfaces A: Physicochemical and Engineering Aspects*, 536 (2018) 198–203.
463 <https://doi.org/10.1016/J.COLSURFA.2017.06.010>.
- 464 Trujillo-Cayado, L.A., García, M.C., Muñoz, J., Alfaro, M.C. Development, rheological
465 properties, and physical stability of d-limonene-in-water emulsions formulated with
466 copolymers as emulsifiers. *J. Appl. Polym. Sci.* (2016).
467 <https://doi.org/10.1002/APP.43838>.
- 468 Trujillo-Cayado, Luis A., García, María C., Santos, Jenifer, Carmona, José A. and Alfaro,
469 María C. Progress in the formulation of concentrated ecological emulsions for
470 agrochemical application based on environmentally friendly ingredients. *ACS*
471 *Sustainable Chem. Eng.*, 5(2017), 4127–4132. [https://doi.org/](https://doi.org/10.1021/acssuschemeng.7b00106)
472 [10.1021/acssuschemeng.7b00106](https://doi.org/10.1021/acssuschemeng.7b00106)
- 473 Xu, D., Zhang, J., Cao, Y., Wang, J., & Xiao, J. *LWT - Food Science and Technology*,
474 66 (2016), 590–597. <https://doi.org/10.1016/j.lwt.2015.11.002>

475

476 **Figure captions**

477 Figure 1. Influence of the processing protocols on the DSD of the primary emulsions at 1
478 day of aging time. Room temperature.

479 Figure 2. Backscattering in whole measuring cell length as a function of aging time for
480 IKA-SL5M emulsion.

481 Figure 3. Delta backscattering at 27 days of aging time as a function of the measuring cell
482 length for all studied systems.

483 Figure 4. Influence of the processing protocol on the creaming index (CI) as a function
484 of aging time.

485 Figure 5. Effect of aging time on the droplet size distributions for SL5M emulsion. Room
486 temperature.

487 Figure 6. Influence of the processing protocol on the Turbiscan Stability Index as a
488 function of aging time.

489 Figure 7. Influence of the pressure applied by M-110P microfluidizer homogenizer on the
490 droplet size distribution. Room temperature.

491 Figure 8. Influence of aging time on the droplet size distribution of the emulsion obtained
492 at 20000 psi.

493 Figure 9. Influence of the applied pressure on the ΔBS as a function of the measuring cell
494 length at 55 days of aging time.

495 Figure 10. Influence of the applied pressure on the creaming index as a function of aging
496 time.

497 Figure 11. Influence of applied pressure on the TSI as a function of aging time.

498

499 **Tables**

500 Table 1. Influence of processing protocol on the mean diameters and span values. Room
501 temperature.

502 Table 2. Influence of processing protocol on the mean diameters and span values. Room
503 temperature.

504 Table 3. Influence of the applied pressure on the creaming rate (ω) and the time of
505 creaming onset ($t_{0,c}$).

506

507 Table 1. Influence of processing protocol on the mean diameters and span values. Room
508 temperature.

	D_{3,2} (μm)	D_{4,3} (μm)	Span
IKA - UT50	2.37 ± 0.07	2.91 ± 0.09	1.215 ± 0.068
UT50	2.04 ± 0.05	2.63 ± 0.07	1.079 ± 0.051
IKA - SL5M	1.98 ± 0.05	2.57 ± 0.07	0.988 ± 0.044
SL5M	1.82 ± 0.06	2.29 ± 0.05	1.164 ± 0.071

509

510

511 Table 2. Influence of processing protocol on the mean diameters and span values. Room
512 temperature.

Pressure (psi)	D_{3,2} (μm)	D_{4,3} (μm)	Span
SL5M	1.82 ± 0.06	2.29 ± 0.05	1.164 ± 0.071
5000	0.74 ± 0.04	1.06 ± 0.06	1.541 ± 0.088
10000	0.68 ± 0.03	1.17 ± 0.07	1.295 ± 0.065
15000	0.59 ± 0.02	0.91 ± 0.05	2.042 ± 0.101
20000	0.52 ± 0.02	1.53 ± 0.08	4.585 ± 0.327
25000	0.78 ± 0.03	1.70 ± 0.08	3.506 ± 0.287

513

514 Table 3. Influence of the applied pressure on the creaming rate (ω) and the time of
515 creaming onset ($t_{0,c}$).

Pressure (psi)	ω (%/day)	$t_{0,c}$ (h)
5000	0.054	0
10000	0.053	125
15000	0.031	355
20000	0.030	436
25000	0.039	136

516

Figure captions

Figure 1. Influence of the processing protocols on the DSD of the primary emulsions at 1 day of aging time. Room temperature

Figure 2. Backscattering in whole measuring cell length as a function of the aging time for IKA-SL5M emulsion

Figure 3. Delta backscattering at 27 days of aging time as a function of the measuring cell length for all studied systems

Figure 4. Influence of the processing protocol on the creaming index (CI) as a function of the aging time

Figure 5. Effect of the aging time on the droplets sizes distributions for SL5M emulsion. Room temperature

Figure 6. Influence of the processing protocol on the Turbiscan Stability Index as a function of the aging time

Figure 7. Influence of the pressure applied by M-110P microfluidizer homogenizer on the droplets sizes distribution. Room temperature

Figure 8. Influence of aging time on the droplet size distribution of the emulsion obtained at 20000psi

Figure 9. Influence of the applied pressure on the ΔBS as a function of the measuring cell length at 55 days of aging time

Figure 10. Influence of the applied pressure on the creaming index as a function of the aging time

Figure 11. Influence of applied pressure on the TSI as a function of the aging time

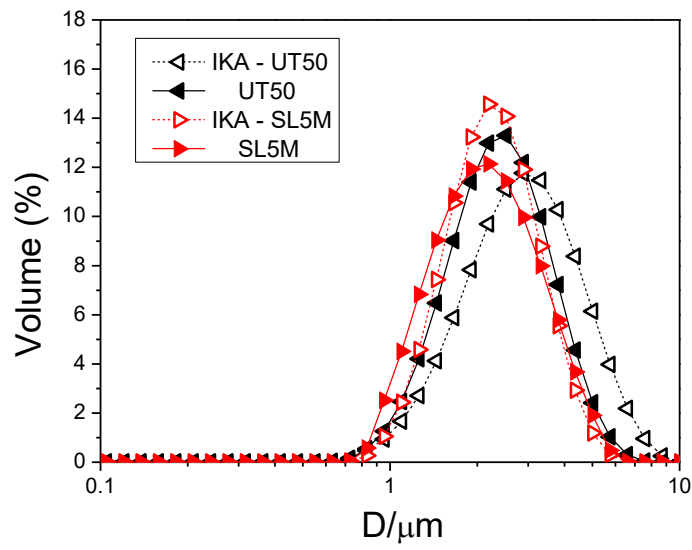


Figure 1. Influence of the processing protocols on the DSD of the primary emulsions at 1 day of aging time. Room temperature.

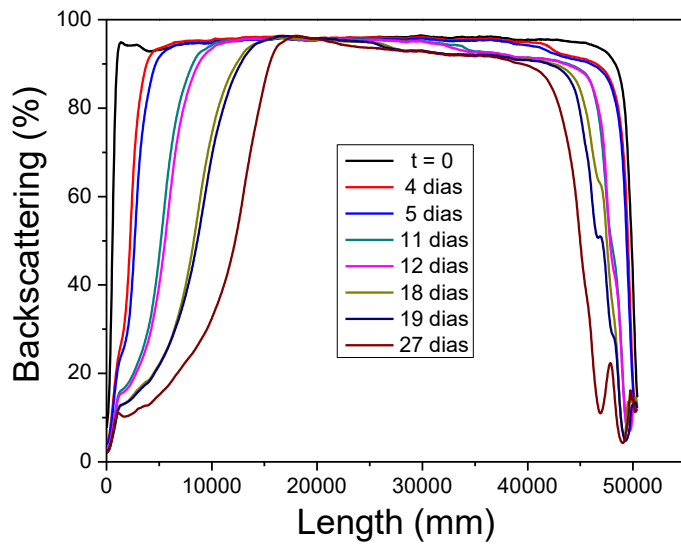


Figure 2. Backscattering in whole measuring cell length as a function of the aging time for IKA-SL5M emulsion

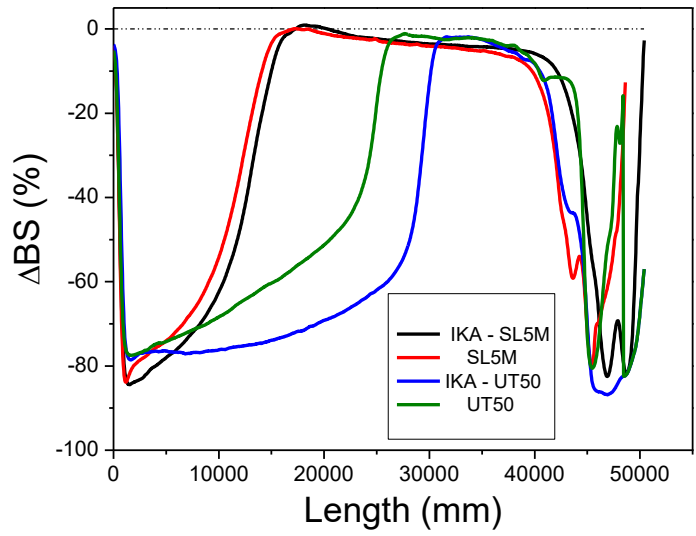


Figure 3. Delta backscattering at 27 days of aging time as a function of the measuring cell length for all studied systems

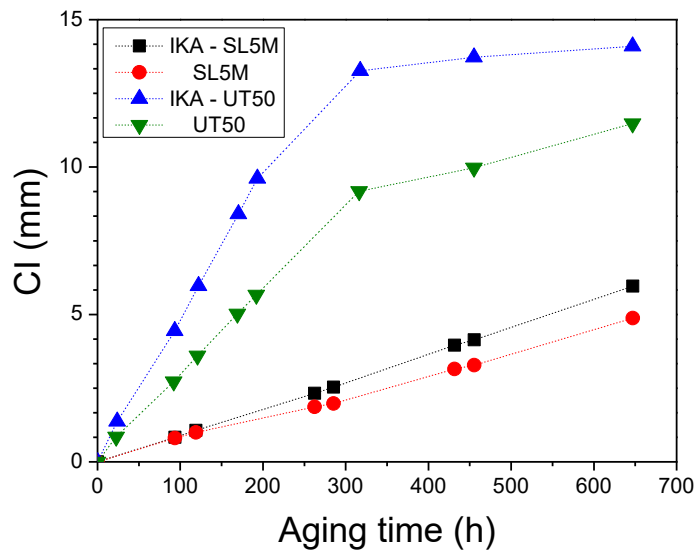


Figure 4. Influence of the processing protocol on the creaming index (CI) as a function of the aging time.

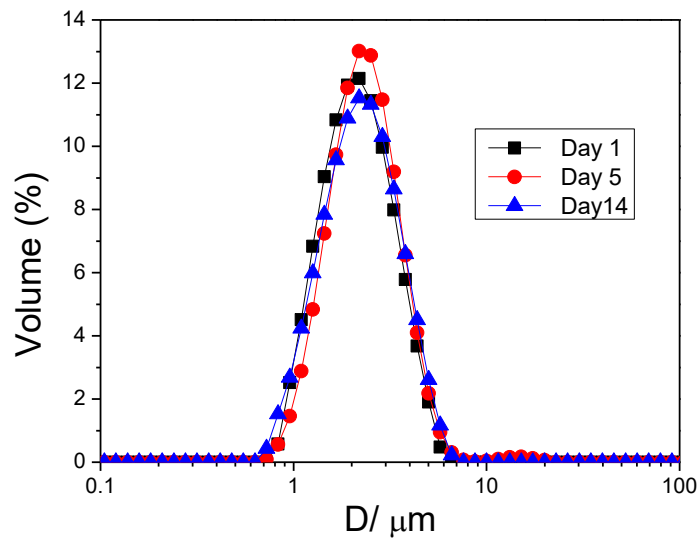


Figure 5. Effect of the aging time on the droplets sizes distributions for SL5M emulsion. Room temperature

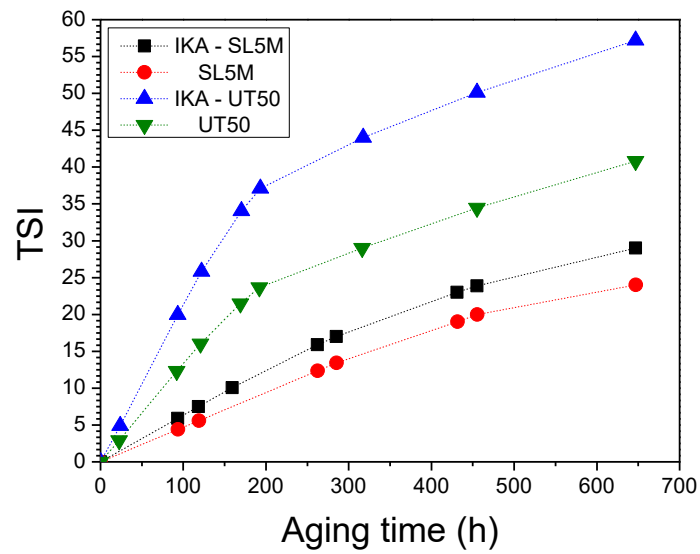


Figure 6. Influence of the processing protocol on the Turbiscan Stability Index as a function of the aging time.

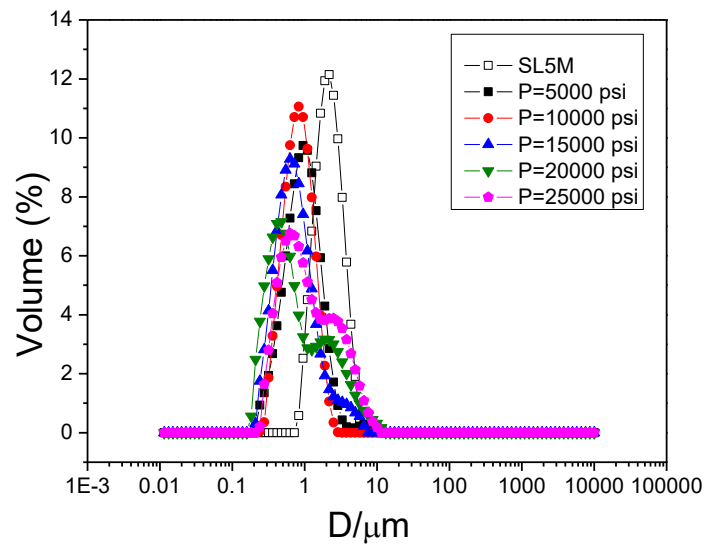


Figure 7. Influence of the pressure applied by M-110P microfluidizer homogenizer on the droplets sizes distribution. Room temperature.

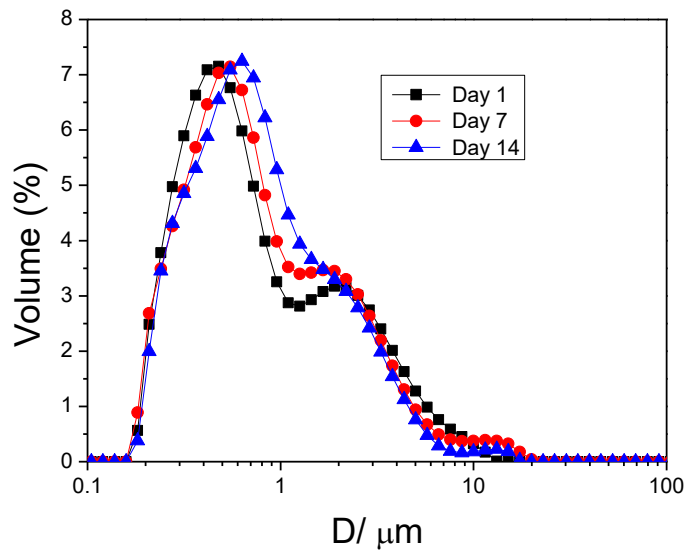


Figure 8. Influence of aging time on the droplet size distribution of the emulsion obtained at 20000psi.

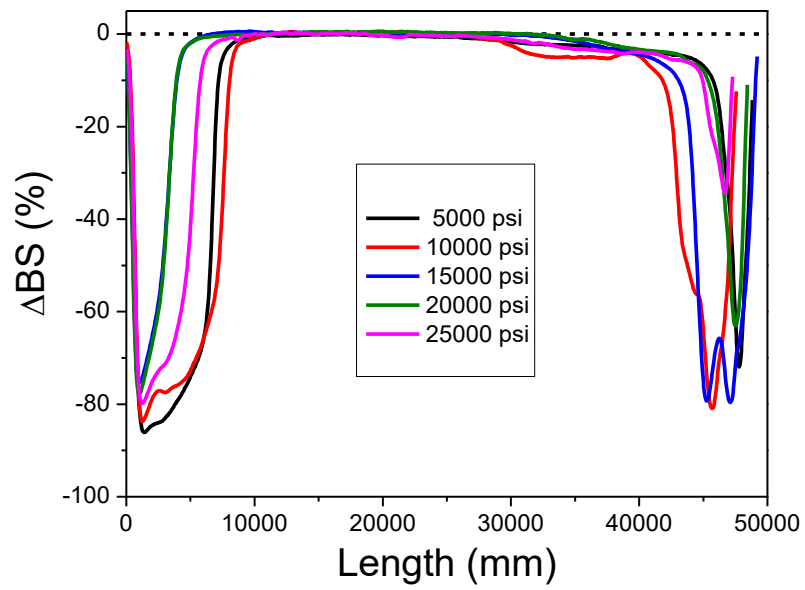


Figure 9. Influence of the applied pressure on the ΔBS as a function of the measuring cell length at 55 days of aging time.

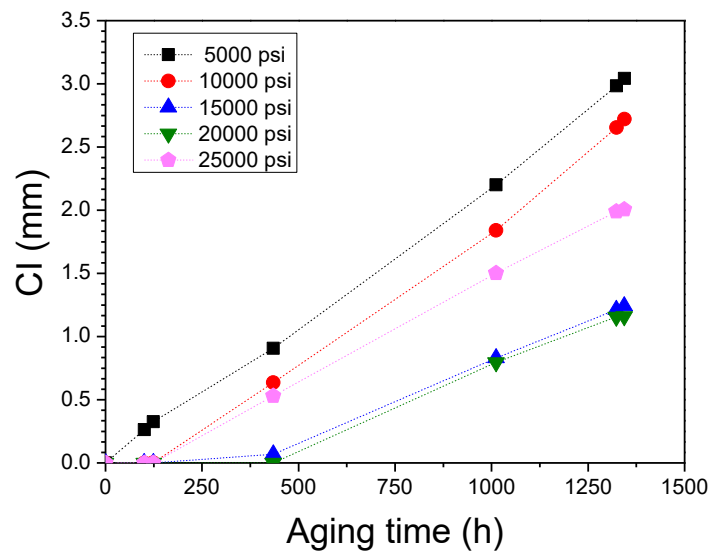


Figure 10. Influence of the applied pressure on the creaming index as a function of the aging time.

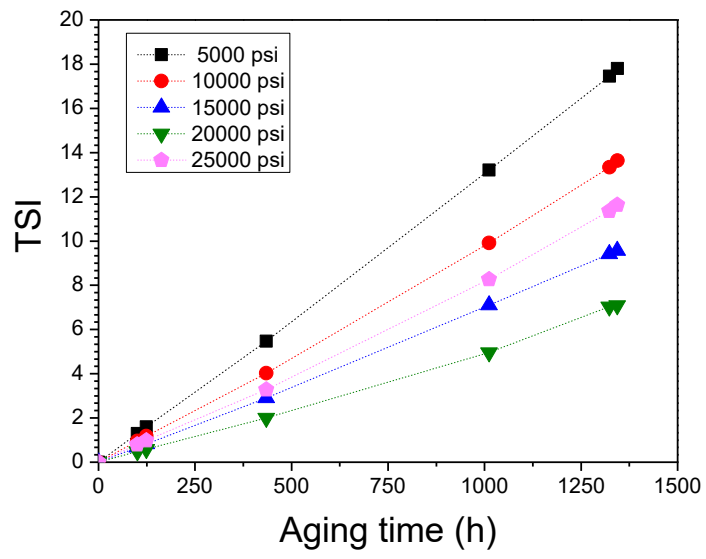


Figure 11. Influence of applied pressure on the TSI as a function of the aging time